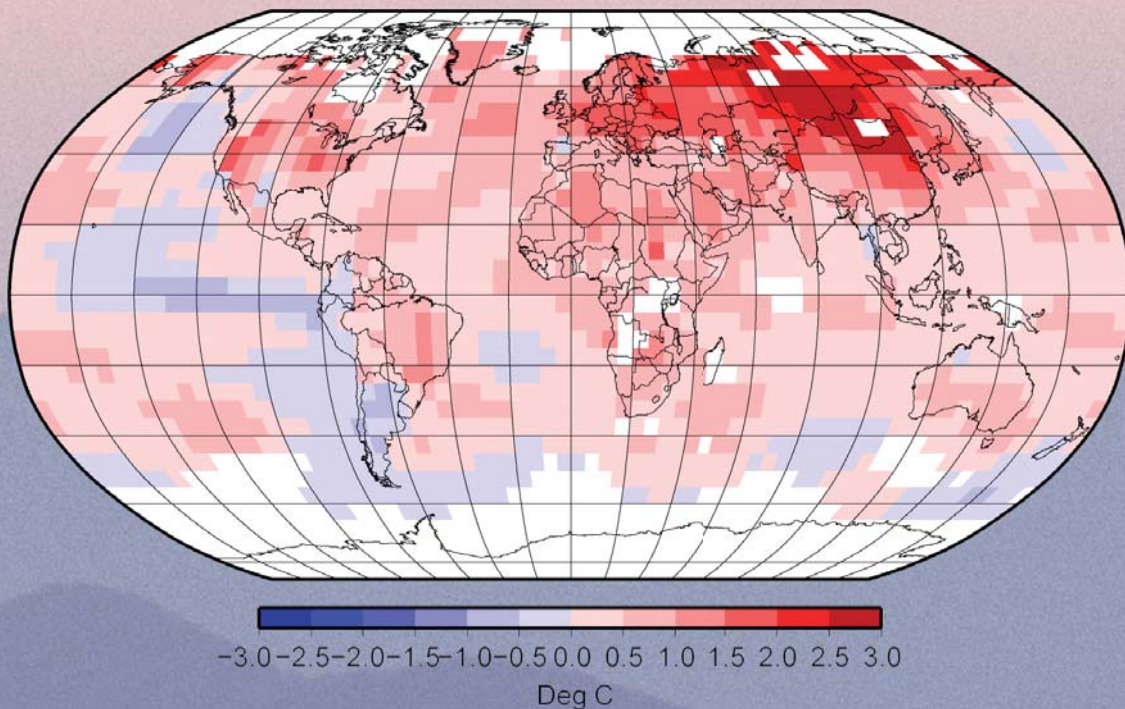


# STATE OF THE CLIMATE IN 2007

D. H. LEVINSON AND J. H. LAWRIMORE, Eds.

ASSOCIATE Eds.: A. ARGUEZ, H. J. DIAMOND, F. FETTERER, A. HORVITZ, J. M. LEVY



Geographic distribution of global surface temperature anomalies in 2007, relative to the 1961 to 1990 average.

Special Supplement to the *Bulletin of the American Meteorological Society*  
Vol. 89, No. 7, July 2008



One last feature of interest in the 2007 salinity field is the anomalously salty water located in the region of the fresh Amazon River plume (Fig. 3.11). The influence of this plume would normally be apparent in relatively fresh conditions to the north and west of the mouth of the Amazon River (the cluster of gray contours near 5°N, 40°W) that reach as far north as Puerto Rico. A salty anomaly observed in this region in 2006, but not 2005 (Arguez et al. 2007), intensified east of 60°W in 2007 (Figs. 3.11 and 3.12). This building salty anomaly may be partly explained by reduced freshwater flow from the Amazon into the ocean during a record drought in the Amazon River basin in 2005 (Shein et al. 2006) that continued, although somewhat moderated into 2006 (Arguez et al. 2007), when some time delay for hydrological and oceanic processes is included.

#### d. Circulation

##### 1) SURFACE CURRENT OBSERVATIONS—R. Lumpkin and G. J. Goni

Global analysis of surface currents indicate that westward current anomalies dominated the equatorial Pacific basin, reflecting the La Niña conditions that developed in the second half of 2007. Long-term trends in eddy kinetic energy reveal that major ocean currents such as the Gulf Stream, Kuroshio, Brazil, and Malvinas Currents are shifting in position and/or strength; these decadal-scale changes may reflect longer-term fluctuations or secular trends.

##### (i) Data and analysis

Near-surface currents are measured in situ by satellite-tracked drifting buoys and by current meters on ATLAS moorings.<sup>1</sup> During 2007, the drifter array ranged in size from a minimum of 1,180 to a maximum of 1,306, with a median size of 1,253 buoys. The moored array consisted of 41 buoys, all but two between 10°S and 21°N. The tropical moored array in the Indian Ocean was expanded considerably in 2007, with several buoys added along 90°E and a new site at 8°S, 67°E. In the Atlantic, the PIRATA array was

expanded and now includes moored current meters at four sites along 23°W. The two nontropical moorings in the observing system are at the Kuroshio Extension Observatory (32°N, 145°E) and Ocean Station Papa (50°N, 145°W) sites.

The findings presented here are based on a combined evaluation of mooring, drifter, and satellite-based surface current measurements. Weekly maps of absolute surface currents and geostrophic current anomalies for 2007 were calculated from a synthesis of in situ observations, near-real-time AVISO gridded altimetry, and NCEP operational winds (Niiler et al. 2003). Anomalies are defined with respect to the January 1993–December 1998 mean. Global analyses using similar methodologies (Bonjean and Lagerloef 2002) and validation of surface currents (Johnson et al. 2007) can be found at [www.oscar.noaa.gov](http://www.oscar.noaa.gov) and [www.aoml.noaa.gov/phod/currents](http://www.aoml.noaa.gov/phod/currents).

##### (ii) Global overview

In 2007, the most dramatic surface current anomalies were westward anomalies spanning the tropical Pacific basin (Fig. 3.13). Maximum annual averaged westward anomalies of 20–25 cm s<sup>-1</sup> were observed at 120°–125°W on the equator, with annual-averaged values of 5–10 cm s<sup>-1</sup> elsewhere. As discussed below, these anomalies were strongest during January–March, but were also sustained from mid-July through the end of 2007. These westward anomalies were associated with the La Niña that developed in the latter half of 2007. Anomalies elsewhere in the World Ocean were caused by energetic mesoscale (60–90 day period) variations or were associated with displacements of currents from their typical positions.

Longer-term trends in EKE were obtained from altimetry-derived sea height anomaly observations, to resolve changes in intensity and location of surface geostrophic currents. These trends were calculated for the observations binned in 1° boxes, calculated over the time period 1993–2007. The global observations indicate that large changes in EKE are occurring in all ocean basins, mainly in the most intense surface currents (Fig. 3.14).

##### (iii) Pacific Ocean

In January–February 2007, westward surface current anomalies developed and intensified across the central equatorial Pacific. During these months, the westward NEC was stronger by 10–30 cm s<sup>-1</sup> across the basin, while the eastward NECC was barely present. The westward anomalies disappeared from the equatorial Pacific by the end of March 2007.

<sup>1</sup> Drifter data are distributed by NOAA/AOML ([www.aoml.noaa.gov/phod/dac/gdp.html](http://www.aoml.noaa.gov/phod/dac/gdp.html)). Moored data are distributed by NOAA/PMEL ([www.pmel.noaa.gov/tao](http://www.pmel.noaa.gov/tao)). Altimetric time series of transports may be viewed online ([www.aoml.noaa.gov/phod/satprod](http://www.aoml.noaa.gov/phod/satprod)). NCEP data provided by the NOAA–CIRES Climate Diagnostics Center ([www.cdc.noaa.gov/](http://www.cdc.noaa.gov/)). AVISO altimetry produced by the CLS Space Oceanography Division as part of the Environmental and Climate EU ENACT project and with support of CNES.

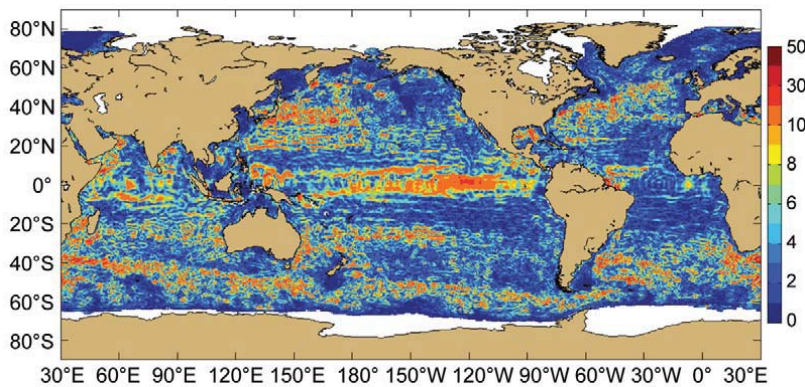


**FIG. 3.13. Amplitude ( $\text{cm s}^{-1}$ ) of 2007 annual averaged surface geostrophic current anomalies.**

Weak eastward anomalies began developing during March, centered at around  $130^{\circ}\text{W}$ , intensified during April, and were very strong by early May at  $110^{\circ}$ – $160^{\circ}\text{W}$ . During May 2007, the center of the eastward anomalies shifted to  $120^{\circ}$ – $150^{\circ}\text{W}$ . Strong off-equatorial ( $3^{\circ}$ – $8^{\circ}\text{N}$ ) westward anomalies developed at  $130^{\circ}$ – $180^{\circ}\text{W}$ . The equatorial eastward anomalies weakened through June.

In July, strong westward anomalies developed in the eastern side of the equatorial Pacific basin ( $90^{\circ}$ – $140^{\circ}\text{W}$ ), a pattern that would grow through the remainder of the year to reflect the development of La Niña conditions. Also in July, eastward anomalies developed in the western side of the basin. These patterns created an anomalous confluence along the equator at  $150^{\circ}$ – $160^{\circ}\text{W}$ . During this period, cold SST anomalies that had previously been confined to the eastern side of the basin began to appear in the Niño-3.4 index region ( $120^{\circ}$ – $170^{\circ}\text{W}$ ) (see also, Figs. 3.2 and 3.20).

Through August, the eastward anomalies diminished, then disappeared. The westward anomalies persisted through this month, and intensified in September to expand and span the basin (Fig. 3.15). Also during this month, the Niño-4 index ( $150^{\circ}\text{W}$ –

$160^{\circ}\text{E}$ ) exhibited a sharp drop in surface temperature partly attributable to westward advection of SST anomalies. The basin-scale pattern of westward equatorial anomalies weakened through October, but persisted in a weakened state through November and December 2007.

The long-term trends in EKE reveal large, positive values in the Kuroshio and Kuroshio Extension region (Fig. 3.14), extending to approximately  $170^{\circ}\text{W}$ , which may be related to the regional intensification of surface currents. Baroclinic instabilities of the Kuroshio are the main source of this EKE (cf. Niiler et al. 2003).

#### (iv) Indian Ocean

During January 2007, the equatorial Indian Ocean exhibited a band of anomalously eastward flow on the eastern half of the basin. Through February, westward anomalies developed in the western half of the basin, and persisted through early March. By April, and persisting through early May, eastward anomalies associated with the equatorial jet were well developed across the equatorial Indian Ocean Basin. This seasonal (monsoon driven) pattern disappeared in May, and in June through September there were no significant current anomalies. In October through November, strong eastward anomalies (the semiannual equatorial jet) developed and propagated across the basin; eastward anomalies persisted in the western third of the basin through December 2007.

The long-term EKE activity in the Agulhas Current region off South Africa (Fig. 3.14) may indicate increasing ring activity. The Agulhas becomes unstable as it separates off the southern tip of South Africa, shedding rings that transport Indian Ocean water into the South Atlantic. This exchange is a significant part of the upper limb of the global meridional overturning circulation, and a decadal-scale increase in this exchange rate may have profound climate implications if verified.

#### (v) Atlantic Ocean

The seasonal reversal of western tropical Atlantic Ocean currents (cf. Lumpkin and Garzoli 2005) was prominent in 2007. Anomalously strong eastward anomalies were seen on the equator in mid-March through

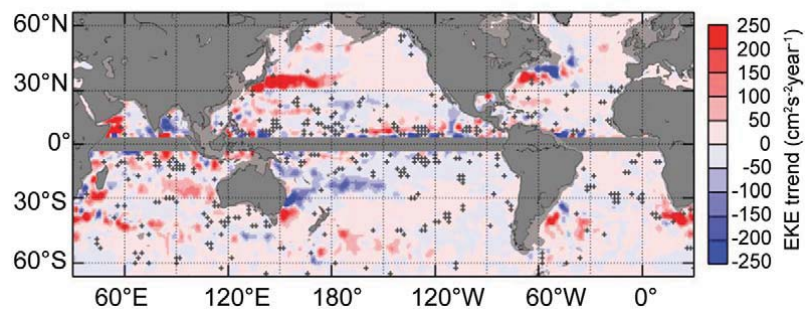


**FIG. 3.14. EKE trend, 1993–2007. Crosses show regions where the confidence levels are  $<67\%$ .**

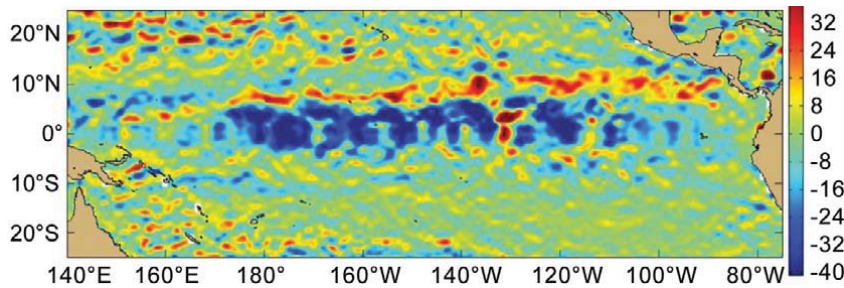


**FIG. 3.15. Zonal geostrophic current anomalies ( $\text{cm s}^{-1}$ ) in mid-Sep 2007 in the tropical Pacific, demonstrating the negative (westward) anomalies associated with the development of the 2007 La Niña.**

early May. By late May, strong westward anomalies had developed at  $\sim 23^\circ\text{W}$  on the equator. These were weak by mid-June, then reintensified in late June through early July, and diminished until they were gone by early August. In September, eastward anomalies were persistent across the central and eastern equatorial Atlantic. This pattern was confined to the Gulf of Guinea by mid-October, and gone entirely by mid-November. Currents in December 2007 were close to their climatological values.

The alternation of positive and negative values in the long-term EKE trend in the northwest North Atlantic and southwest South Atlantic (Fig. 3.14) are indicative of the variability in the subtropical gyres. This change in the South Atlantic is consistent with a shift to the south of the Brazil Current jet (Fig. 3.16). The Brazil Current runs south along the coast until it collides head-on with the northward Malvinas Current; both subsequently turn eastward. During the last 15 yr, the location where the Brazil Current separates from the continental shelf break has moved  $2^\circ$  to the south, possibly indicating an expansion of the South Atlantic wind-driven subtropical gyre (Goni et al. 2008).

## 2) THE MERIDIONAL OVERTURNING CIRCULATION—M. O. Baringer and C. S. Meinen

The global ocean–atmosphere system can be thought of as a massive heat engine, redistributing heat from the sun and in so doing causing both short-term weather systems and long-term changes in climate. In the ocean, the so-called MOC is largely responsible for the redistribution of heat, mass and freshwater within the global ocean system. Specifically, the MOC is defined here as the maximum of the zonal integral of mass transport

of the large-scale, low-frequency, full-depth ocean circulation. The strengths of the overturning circulations in different basins are directly related to the strength of the heat transport (see Baringer and Meinen 2007 for more discussion). There are several available estimates of the steady-state global mass and heat transport based on inverse model calculations (Lumpkin and Speer 2007; Ganachaud and Wunsch 2003; Talley

2003). Recently, there have been only a few attempts to look at long-term changes in the MOC from direct observations. Bryden et al. (2005) postulate a 30% reduction in the MOC transport between the 1950s and the present day; however, that analysis is based on a very limited dataset (essentially five “snapshot” hydrographic sections). Other recent work using cross-basin hydrographic sections along  $48^\circ\text{N}$  in the Atlantic suggest conflicting conclusions relative to the state of the thermohaline circulation. In particular Koltermann et al. (1999) show large variability of the MOC that, they conclude, is related to the strength of Labrador Sea Water production, with larger (smaller) MOC transport corresponding to less (more) Labrador Sea Water export. More recently these data have been re-analyzed to formally test the hypothesis that the MOC circulation is steady. Lumpkin et al. (2008) find that a steady MOC over the same time period could not be ruled out based on the uncertainty in determining the barotropic circulation. It is also noteworthy that the Bryden et al. (2005) suggestion that the thermohaline circulation has declined by 30% over the past 50 yr represents a much higher rate of change than predicted in coupled climate model simulations (e.g., Schmittner

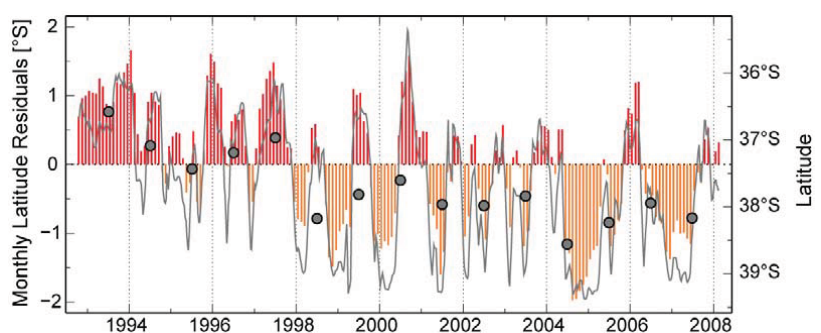


**FIG. 3.16. Latitude of separation of the Brazil Current from the continental shelf (black line), monthly anomalies of the separation (vertical bars), and mean annual values (circles) calculated from AVISO altimetry, showing a mean shift to the south of approximately  $2^\circ$ . (From Goni et al. 2008.)**